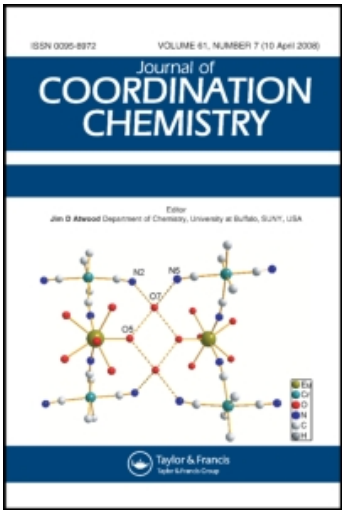

Journal of Coordination Chemistry
Publication details, including instructions for authors and subscription information:
http://www.informaworld.com/smpp/title~content=t713455674

Vanadium(IV)-substituted tungstoantimonate $[Sb_2W_{20}(VO)_2(H_2O)_4O_{70}]^{10-}$: synthesis, crystal structure and electrochemistry

Li-Hua Bi[a]; Bao Li[a]; Li-Xin Wu[a]
[a] College of Chemistry, State Key Laboratory of Supramolecular Structure and Materials, Jilin University, Changchun 130012, P.R. China

First published on: 01 October 2010

To cite this Article Bi, Li-Hua , Li, Bao and Wu, Li-Xin(2009) 'Vanadium(IV)-substituted tungstoantimonate $[Sb_2W_{20}(VO)_2(H_2O)_4O_{70}]^{10-}$: synthesis, crystal structure and electrochemistry', Journal of Coordination Chemistry, 62: 4, 531 — 539, First published on: 01 October 2010 (iFirst)
To link to this Article: DOI: 10.1080/00958970802287199
URL: http://dx.doi.org/10.1080/00958970802287199

Journal of Coordination Chemistry
Vol. 62, No. 4, 20 February 2009, 531–539

Taylor & Francis
Taylor & Francis Group

Vanadium(IV)-substituted tungstoantimonate $[Sb_2W_{20}(VO)_2(H_2O)_4O_{70}]^{10-}$: synthesis, crystal structure and electrochemistry

LI-HUA BI*, BAO LI and LI-XIN WU

College of Chemistry, State Key Laboratory of Supramolecular Structure and Materials, Jilin University, Changchun 130012, P.R. China

(*Received 13 February 2008; in final form 30 April 2008*)

A vanadium(IV)-substituted tungstoantimonate, $K_8Na_2[Sb_2W_{20}(VO)_2(H_2O)_4O_{70}]\cdot 18.5H_2O$ (**1**), has been synthesized in aqueous solution and characterized by IR, UV–Vis, elemental analysis, TG and X-ray single-crystal diffraction analysis. The structure of **1** was composed of two V(IV) ions linked to a $[Sb_2W_{20}O_{70}]^{14-}$ fragment via V–O(W) bonds; the anions are connected by K^+ to construct a two-dimensional network complex. The electrochemical behavior of **1** was investigated in buffer solution (pH 2.5) by cyclic voltammetry. In the potential range between −0.7 and 0.9 V, the compound exhibits successive redox processes of the addenda atoms (W) in a negative potential range, and also redox originating from the substituted atom (V) at a more positive potential. Compound **1** has good electrocatalytic activity towards the reduction of iodate.

Keywords: Tungstoantimonate; Vanadium; Dimeric polyoxoanion; Network complex; Electrocatalytic; Iodate

1. Introduction

Transition metal substituted polyoxometalates (TMSPs) have attracted attention because of their highly tunable nature, fascinating properties and potential applications in catalysis, material science, and medicine [1–3]. TMSPs have long been recognized as inorganic analogues of metalloporphyrin complexes. However, the TMSPs have distinct advantages over their counterparts, for they are rigid, hydrolytically stable and thermally robust [4, 5]. TMSPs constitute the largest subfamily of polyanions [6–8]. A large number of novel TMSPs with diverse compositional range and unexpected shapes and sizes are still being discovered [9–12]. However, considering that formation of polyanions occurs via self-assembly, the discovery of TMSPs with fundamentally novel structures or different composition continues to be a focus of ongoing research.

Sb^{III}-containing POMs with the lone pair of electrons on the heteroatom do not allow the closed Keggin unit to form, resulting in unexpected structures, e.g. $[NaSb_9W_{21}O_{86}]^{18-}$, $[Na_2Sb_8W_{36}O_{132}(H_2O)_4]^{22-}$ [13, 14]. The polyoxoanions, $[Sb^{III}W_9O_{33}]^{9-}$

*Corresponding author. Email: bilihua@email.jlu.edu.cn

ISSN 0095-8972 print/ISSN 1029-0389 online © 2009 Taylor & Francis
DOI: 10.1080/00958970802287199

and $[Sb_2W_{22}O_{74}(OH)_2]^{12-}$, are the most studied systems in the Sb-containing POMs [14, 15]. The compounds, $[M_2(H_2O)_6(WO_2)_2(\beta\text{-}SbW_9O_{33})_2]^{(14-2n)-}$ ($M^{n+} = Fe^{3+}$, Co^{2+}, Mn^{2+}, Ni^{2+}, Cu^{2+}, Zn^{2+}), have been reported [14, 15]. Recently, Proust reported the organo-Ru supported tungstoantimonate $[Sb_2W_{20}O_{70}\{Ru(p\text{-cymene})\}_2]^{10-}$ [16].

Very recently, we reported the electrochemical behavior of $[Sb_2W_{20}Fe_2O_{70}(H_2O)_6]^{8-}$ and its multilayer films fabricated onto GCE surface by layer-by-layer self assembly [17]. Here we report the synthesis, crystal structure and electrochemistry of a vanadium(IV)-substituted tungstoantimonate $[Sb_2W_{20}(VO)_2(H_2O)_4O_{70}]^{10-}$.

2. Experimental

2.1. *Chemicals and methods*

All chemicals were high-purity grade, purchased from Aldrich and used as received. Deionized water was used throughout. $[Sb_2W_{22}O_{74}(OH)_2]^{12-}$ was synthesized according to the literature and characterized by IR spectra [14]. Elemental analysis was performed on a PLASMA-SPEC (I) ICP atomic emission spectrometer. IR spectra were recorded in the range 400–4000 cm^{-1} on an Alpha Centauri FT/IR spectrophotometer using KBr pellets. Thermogravimetric analysis was carried out on a TA Instruments SDT Q600 thermobalance with a 100 mL min^{-1} flow of nitrogen; the temperature was ramped from 20 to 800°C at a rate of 5°C min^{-1}. UV–Vis absorption spectrum was obtained using a Cintra 10e UV–Vis spectrometer. The X-ray powder diffraction (XRD) was performed on a Siemens D5005 diffractometer with graphite-filtered Cu-Kα radiation. Electrochemical measurements were carried out on CHI 660C electrochemical workstation at room temperature under nitrogen atmosphere. A three electrode electrochemical cell was used with a GCE as the working electrode, a platinum wire as the counter and a Ag/AgCl reference electrode. Buffer solutions were prepared from the following solutions, 0.5 M $Na_2SO_4 + H_2SO_4$ (pH 1.5–3.5) and 0.5 M NaAc + HAc (pH 4.0–6.0). Formal potentials (E_f) were estimated as average values of anodic (E_{pa}) and cathodic (E_{pc}) peak potentials, i.e. $E_f = (E_{pa} + E_{pc})/2$.

2.2. *Synthesis*

$K_8Na_2[Sb_2W_{20}(VO)_2(H_2O)_4O_{70}] \cdot 18.5H_2O$ (1). A 1.0 g (0.15 mmol) sample of $Na_{12}[Sb_2W_{22}O_{74}(HO)_2]$ was added with stirring to a solution of 0.05 g (0.31 mmol) of $VOSO_4$ in 20 mL water. This solution was heated to 80°C for 30 min and then cooled to room temperature and filtered. 1.0 mL of 1.0 M KCl was then added. This solution was allowed to evaporate in an open beaker at room temperature. A brown crystalline product started to appear after one week. Evaporation was continued until the solvent approached the solid product (yield 0.62 g, 70%). Anal. Calcd (found) for $K_8Na_2[Sb_2W_{20}(VO)_2(H_2O)_4O_{70}] \cdot 18.5H_2O$: K, 5.2 (4.9); Na, 0.77 (0.75); Sb, 4.1 (4.0); W, 61.9 (61.5); V, 1.7 (1.6); H_2O, 6.8 (7.6). IR (KBr pellet): 955 (s), 885 (sh), 855 (m), 801 (s), 753 (s). UV–Vis (H_2O): 659 nm, 263 nm, 200 nm.

Table 1. Crystal data and structure refinement for **1**.

Empirical formula	$K_8Na_2O_{94.5}Sb_2V_2W_{20}$
Formula weight	5938.52
Temperature (K)	293(2)
Wavelength (Å)	0.71073
Crystal system	Monoclinic
Space group	$P2_{1/c}$
Unit cell dimensions (Å, °)	
a	19.039(4)
b	11.886(3)
c	22.563(3)
α	90.00
β	118.650 (10)
γ	90.00
Volume (Å^3)	4480.8(16)
Z	1
D_{Calcd} (Mg m^{-3})	4.402
Absorption coefficient (mm^{-1})	26.842
$F(000)$	5206
Data/restraints/parameters	10209/36/619
Goodness-of-fit on F^2	1.091
Final R indices [$I>2\sigma(I)$]	$R_1=0.0281$, $wR_2=0.0580$
R indices (all data)	$R_1=0.0339$, $wR_2=0.0598$
Largest diff. peak and hole (eÅ^{-3})	3.598 and −1.535

X-ray single-crystal data for **1** was set on the end of a glass capillary for indexing and intensity data collection at 293 K on a Rigaku/MSC mercury diffractometer with graphite monochromated Mo-Kα radiation ($\lambda=0.71073$ Å). Direct methods were used to solve the structures and to locate the heavy atoms (SHELXS-97). Remaining atoms were found from successive difference maps (SHELXL-97). All the non-hydrogen atoms were refined anisotropically. Further details of the X-ray structural analysis are given in table 1.

3. Results and discussion

3.1. *Synthesis and structure*

We have synthesized the V(IV)-substituted dimeric tungstoantimonate(III) $[Sb_2W_{20}(VO)_2(H_2O)_4O_{70}]^{10-}$ as a mixed potassium-sodium salt. This polyanion consists of two lacunary β-B-$[Sb^{III}W_9O_{33}]^{9-}$ Keggin fragments linked via two V(IV) atoms and two WO_2 groups leading to a structure with nominal C_2 symmetry (see figures 1, 2 and 3). The polyanion was synthesized by interaction of $VOSO_4$ with the Krebs-type polyanion precursor $[Sb_2W_{22}O_{74}(OH)_2]^{12-}$ in aqueous medium heating to 80°C, exchanging two tungsten-oxo groups for V. This substitution has been observed in other transition-metal-substituted tungstoantimonate $[M_2(H_2O)_6(WO_2)_2(\beta\text{-}SbW_9O_{33})_2]^{(14-2n)-}$ ($M^{n+}=Fe^{3+}$, Co^{2+}, Mn^{2+}, Ni^{2+}, Cu^{2+}, Zn^{2+}).

In 1997, Krebs *et al*. first described the structural type of $[Sb_2W_{22}O_{74}(HO)_2]^{12-}$, which is composed of two identical β-B-$[Sb^{III}W_9O_{33}]^{9-}$ fragments joined by four WO_6 octahedra, among which the two external ones display a facial $\{WO_2(OH)\}^+$ arrangement [14]. Recent studies by the same authors showed that two *fac*-$\{WO_2(OH)\}^+$ groups can be

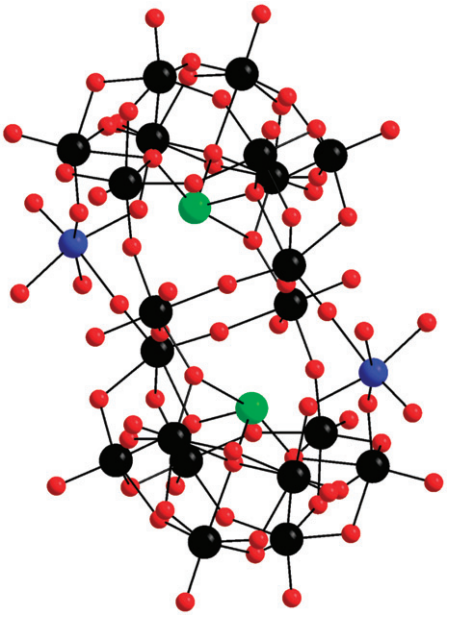

Figure 1. Ball and stick representation of **1**. The balls represent tungsten (black), antimony (green), vanadium (blue), oxygen (red; color online only).

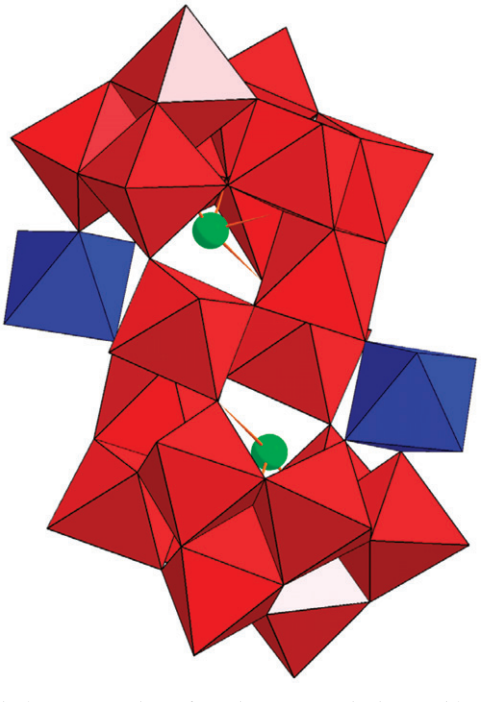

Figure 2. Ball and polyhedral representation of **1**. The VO_6 octahedra are blue (color online only) and the WO_6 octahedra are red. The ball represents antimony (green).

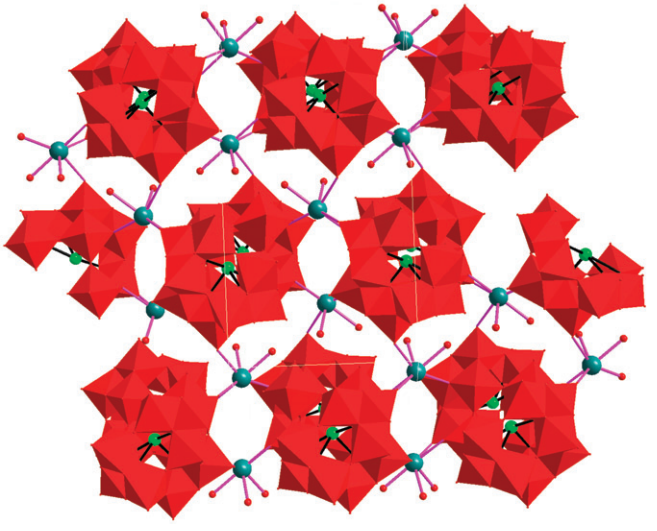

Figure 3. Combined polyhedral/ball-and-stick representation of the two-dimensional network structure of **1**. The color codes for the online version are as follows: WO_6 and VO_6 octahedral are red; the ball represents antimony (green), potassium (gray), oxygen (red).

replaced by various $M^{n+}(H_2O)_3$ units forming polyoxoanions $[M_2(H_2O)_6(WO_2)_2(\beta\text{-}SbW_9O_{33})_2]^{(14-2n)-}$ ($M^{n+} = Fe^{3+}$, Co^{2+}, Mn^{2+}, Ni^{2+}, Cu^{2+}, Zn^{2+}) [14, 15]. Very recently, Proust reported that organo-Ru moieties replaced the two *fac*-$\{WO_2(OH)\}^+$ fragments resulting in the new tungstoantimonate $[Sb_2W_{20}O_{70}\{Ru(p\text{-cymene})\}_2]^{10-}$ [16]. It has also been possible to substitute the antimony(III) heteroatom by bismuth(III). In 1999, the same authors reported the isostructural tungstobismutate $[Bi_2W_{22}O_{74}(HO)_2]^{12-}$ and its derivatives $[M_2(H_2O)_6(WO_2)_2(\beta\text{-}BiW_9O_{33})_2]^{(14-2n)-}$ ($M^{n+} = Fe^{3+}$, Co^{2+}, Mn^{2+}, Ni^{2+}, Cu^{2+}, Zn^{2+}) [15].

The structure of the polyanion of **1** is closely related to $[Sb_2W_{22}O_{74}(OH)_2]^{12-}$ and the transition-metal-substituted heteropolyanion clusters $[M_2(H_2O)_6(WO_2)_2(\beta\text{-}SbW_9O_{33})_2]^{(14-2n)-}$ ($M^{n+} = Fe^{3+}$, Co^{2+}, Mn^{2+}, Ni^{2+}, Cu^{2+}, Zn^{2+}) [14, 15] and can be described as two $[VO(H_2O)_2]^{2+}$ species replacing two *fac*-$\{WO_2(OH)\}^+$ moieties to form $[Sb_2W_{20}(VO)_2(H_2O)_4O_{70}]^{10-}$. The V(IV) atoms are bound to chemically inequivalent oxygens with V–O distances from 1.972(7) to 2.194(6) Å; one belongs to a complete $\{W_3O_{13}\}$ triad of one $\{SbW_9O_{33}\}$ unit, while the other two belong to two different $\{W_3O_{13}\}$ triads of the second $\{SbW_9O_{33}\}$ unit. In addition, one is the terminal oxygen with bond distance of 1.609(6) Å, while the other positions are two aquo ligands with distances of 2.039(6) and 2.049(8) Å. The same coordination mode has been observed in $[Bi_2W_{20}(VO)_2(H_2O)_4O_{70}]^{10-}$ [18].

The bond lengths and bond angles in the polyanion of **1** are not unusual. Bond-valence sum calculations [19] indicate that there are no protonation sites and the charge of V is +4 (the bond valence sum for V^{4+} is $s = 4.06$), therefore the charge of the polyanion of **1** must be −10. In the solid state, the negative charges of **1** are balanced by 8 potassium and 2 sodium ions, all crystallographically identified, but K4, K5 and K6 only occupy 0.5, 0.3 and 0.2 of the sites based on the rationality of their atomic thermal displacement parameters. Disorder of some alkali ions is a common problem in polyanion chemistry.

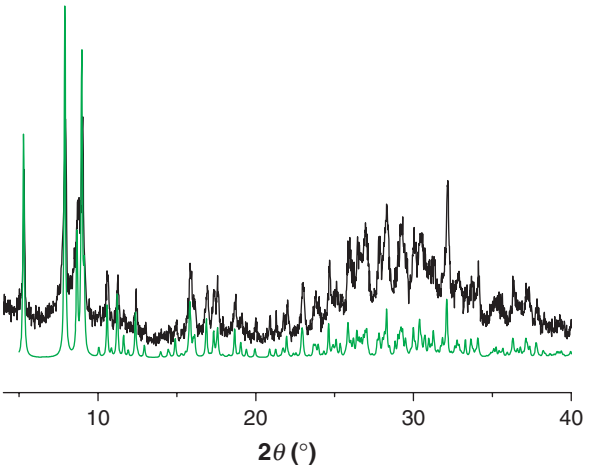

Figure 4. X-ray powder diffraction (XRD) pattern of **1**: measured (black) and produced from single crystal cif. file (green; color online only).

Another interesting feature of **1** is that the dimeric tungstoantimonate anion $[Sb_2W_{20}(VO)_2(H_2O)_4O_{70}]^{10-}$ moieties interconnect each other via K2 to form an infinite 2D network. First, the K2 ion is coordinated by two oxygens [K2–O20 (W5, W9): 2.815 Å; K2-O34 (W10): 2.768 Å] from two neighboring polyoxoanions to form an infinite 1D chainlike; second, the K2 is coordinated by oxygen (K2–O24 (W6): 2.868 Å) from the neighboring 1-D chainlike structure to form an infinite 2-D network, a scarcely observed structure in POMs chemistry.

In addition, in order to verify the purity of the compound we performed powder X-ray diffraction (PXRD) of **1** and compared the pattern with that from crystal structure cif file, as shown in figure 4. It can be seen that all the diffraction peaks are consistent, indicating that **1** is pure.

3.2. *Electrochemistry*

The potassium–sodium salt **1** is a water-soluble brown crystal. We employed UV–Visible spectra to monitor the stability of **1** as a function of pH and time overnight, which is enough for electrochemical characterization of **1**. The results indicate that **1** is stable between pH 2 and 5; the following electrochemical experiments were run at pH 2.5.

Cyclic voltammetric behavior of **1** in pH 2.5 (0.5 M $Na_2SO_4 + H_2SO_4$) buffer with different negative potential limits are presented in figure 5. Three well-defined redox waves from the polyanion are seen between +0.9 and −0.7 V on a GCE and the mean peak potentials $E_{1/2} = (E_{pa} + E_{pc})/2$ are −0.58 V (I–I′), −0.49 V (II–II′) and 0.58 V (III–III′) (*vs.* Ag/AgCl), respectively. The two peaks of I–I′ and II–II′ are attributed to $W^{VI/V}$ redox processes and peak III–III′ to $V^{V/IV}$ redox. Figure 6 shows the cyclic voltammograms (CVs) of **1** in same pH medium at different scan rates; the peak currents of **1** are almost proportional to the square root of the scan rates up to 1000 mV s^{-1}, taking the oxidation peak III and the reduction peak II′ of **1** as representative (shown in the inset of figure 6). This indicates that the redox waves are diffusion-controlled redox processes.

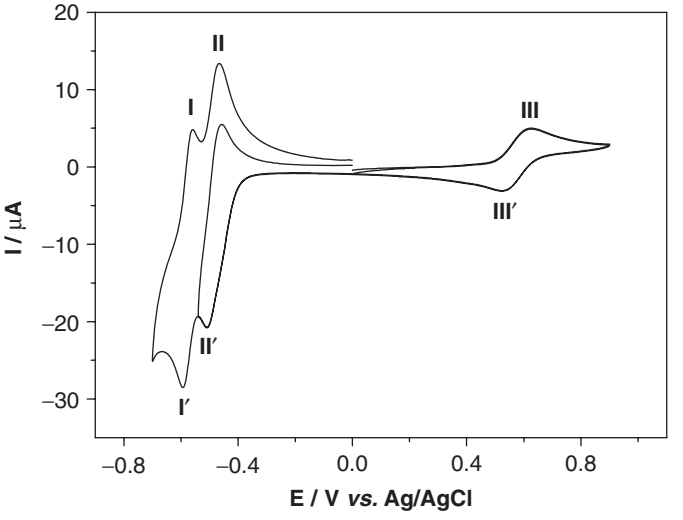

Figure 5. CVs of 0.49 mM **1** in 0.5 M $Na_2SO_4 + H_2SO_4$ at pH 2.5 with different potential limits: −0.54 V and −0.7 V. Scan rate: 50 mV s^{-1}.

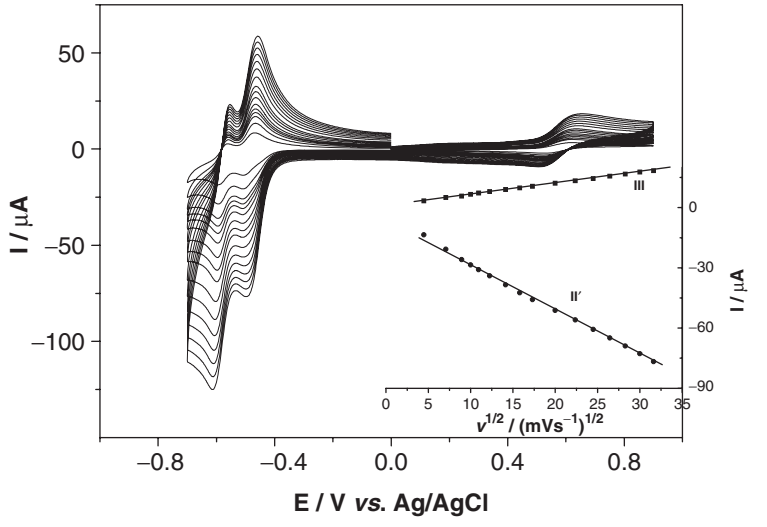

Figure 6. CVs of 0.49 mM **1** in 0.5 M $Na_2SO_4 + H_2SO_4$ at pH 2.5 at scan rates of 20, 50, 80, 100, 120, 150, 200, 250, 300, 400, 500, 600, 700, 800, 900 and 1000 mV s^{-1}. The inset shows the relationship of the square root of scan rates *vs.* the oxidation peak currents of V and reduction peak currents of W.

We also investigated the electrocatalytic reduction of IO_3^- at pH 2.5. Reduction of IO_3^- is irreversible at a bare carbon electrode with large overpotential. In the present experiments, **1** shows good catalytic response towards reduction of IO_3^-. Figure 7 shows the CVs of **1** in solution containing IO_3^- at various concentrations. It is clear that the first reduction peak becomes substantially increased on addition of IO_3^-, while the oxidation peak is decreased. Apparently, the tungsten-oxo species of **1** catalyze the electrochemical reduction of IO_3^-.

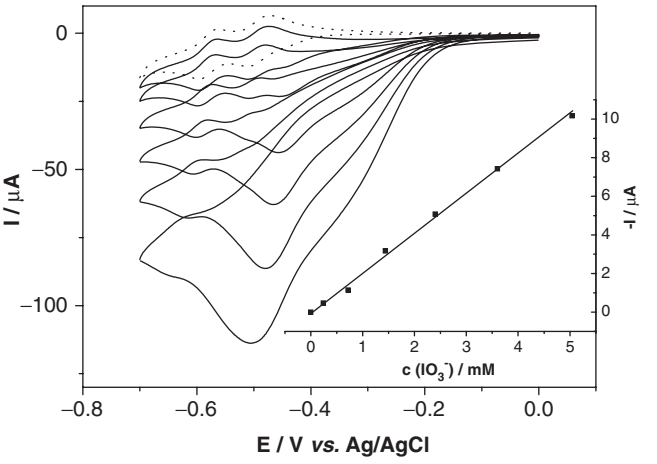

Figure 7. The CVs of 0.61 mM **1** in 0.5 M $Na_2SO_4 + H_2SO_4$ (pH 2.5) buffer solutions at 10 mV s^{-1} in the presence of iodate. The inset shows the catalytic currents caused by the first cathodic wave of W *vs.* concentrations of iodate at various concentrations: 0, 0.24, 0.72, 1.44, 2.4, 3.6 and 5.04 mM.

4. Conclusion

A dimeric V(IV)-substituted tungstoantimonate $K_8Na_2[Sb_2W_{20}(VO)_2(H_2O)_4O_{70}] \cdot 18.5H_2O$ has been synthesized in aqueous solution and structurally characterized. The polyoxoanion in **1** consists of two V(IV) atoms linked to a Krebs-type polyanion $[Sb_2W_{20}O_{70}]^{14-}$, and it is further connected by K^+ to a two-dimensional network structure. The electrochemical properties of the compound demonstrate that it shows good electrocatalytical activities for reduction of IO_3^-.

References

[1] (a) M.T. Pope, A. Müller. *Polyoxometalates: From Platonic Solid to Anti-retroviral Activity*, Kluwer Academic Publishers, Dordrecht (1994); (b) M.T. Pope, A. Müller. *Polyoxometalate Chemistry: From Topology Via Self-Assembly to Applications*, Kluwer, Dordrecht, The Netherlands (2001); (c) C.L. Hill. *J. Mol. Catal. A-Chem.*, **262**, 1 (2007); (d) D.L. Long, E. Burkholder, L. Cronin. *Chem. Soc. Rev.*, **36**, 105 (2007).

[2] (a) C.L. Hill. *Chem. Rev.*, **98**, 1 (1998); (b) M.T. Pope, A. Müller. *Angew. Chem., Int. Ed. Engl.*, **30**, 34 (1991); (c) T. Yamase, M.T. Pope. *Polyoxometalate Chemistry for Nano-Composite Design*, Kluwer, Dordrecht, The Netherlands (2002); (d) J.J. Borrás-Almenar, E. Coronado, A. Müller, M.T. Pope. *Polyoxometalate Molecular Science*, Kluwer, Dordrecht, The Netherlands (2004).

[3] (a) W. Qi, H.L. Li, L.X. Wu. *Adv. Mater.*, **19**, 1983 (2007); (b) H.L. Li, H. Sun, W. Qi, M. Xu, L.X. Wu. *Angew. Chem. Int. Ed.*, **46**, 1300 (2007); (c) H. Zhang, X.K. Lin, Y. Yan, L.X. Wu. *Chem. Commun.*, 4575 (2006).

[4] M.T. Pope. *Heteropoly and Isopoly Oxometalates*, Springer-Verlag, Berlin (1983).

[5] C.L. Hill, R.B. Brown. *J. Am. Chem. Soc.*, **108**, 536 (1986).

[6] (a) Z.M. Zhang, E.B. Wang, Y.G. Li, Y.F. Qi, H.Q. Tan. *J. Mol. Struct.*, **843**, 128 (2007); (b) Z.M. Zhang, Y.F. Qi, C. Qin, Y.G. Li, E.B. Wang, X.L. Wang, Z.M. Su, L. Xu. *Inorg. Chem.*, **46**, 8162 (2007); (c) Z.M. Zhang, Y.G. Li, E.B. Wang, Y.F. Qi, X.L. Wang, C. Qin, H.Q. Tan. *J. Mol. Struct.*, **831**, 69 (2007); (d) Z.M. Zhang, Y.G. Li, E.B. Wang, X.L. Wang, C. Qin, H.Y. An. *Inorg. Chem.*, **45**, 4313 (2006).

[7] (a) M.T. Pope. *Compr. Coord. Chem. II*, **4**, 635 (2003); (b) C.L. Hill. *Compr. Coord. Chem. II*, **4**, 679 (2003).

[8] (a) L.H. Bi, U. Kortz, B. Keita, L. Nadjo, L. Daniels. *Eur. J. Inorg. Chem.*, **15**, 3034 (2005); (b) L.H. Bi, U. Kortz, S. Nellutla, A.C. Stowe, J. Van Tol, N.S. Dalal, B. Keita, L. Nadjo. *Inorg. Chem.*, **44**, 896 (2005); (c) L.H. Bi, U. Kortz. *Inorg. Chem.*, **43**, 7961 (2004); (d) L.H. Bi, U. Kortz, B. Keita, L. Nadjo, H. Borrmann. *Inorg. Chem.*, **43**, 8367 (2004); (e) L.H. Bi, M. Reicke, U. Kortz, B. Keita, L. Nadjo, R.J. Clark. *Inorg. Chem.*, **43**, 3915 (2004); (f) L.H. Bi, E.B. Wang, J. Peng, R.D. Huang, L. Xu, C.W. Hu. *Inorg. Chem.*, **39**, 671 (2000).

[9] (a) N.H. Nsouli, S.S. Mal, M.H. Dickman, U. Kortz, B. Keita, L. Nadjo, J.M. Clemente-Juan. *Inorg. Chem.*, **46**, 8763 (2007); (b) B.S. Bassil, M.H. Dickman, I. Romer, B. von der Kammer, U. Kortz. *Angew Chem. Int. Ed.*, **46**, 6192 (2007); (c) B.S. Bassil, M.H. Dickman, M. Reicke, U. Kortz, B. Keita, L. Nadjo. *Dalton Trans.*, 4253 (2006); (d) B.S. Bassil, U. Kortz, A.S. Tigan, J.M. Clemente-Juan, B. Keita, P. de Oliveira, L. Nadjo. *Inorg. Chem.*, **44**, 9360 (2005); (e) B.S. Bassil, S. Nellutla, U. Kortz, A.C. Stowe, J.V. Tol, N.S. Dalal, B. Keita. *Inorg. Chem.*, **44**, 2659 (2004).

[10] (a) P. Mialane, A. Dolbecq, J. Marrot, E. Riviere, F. Secheresse. *Chem.-Eur. J.*, **11**, 1771 (2005); (b) P. Mialane, A. Dolbecq, F. Secheresse. *Chem. Commun.*, 3477 (2006); (c) L. Lisnard, P. Mialane, A. Dolbecq, J. Marrot, J.M. Clemente-Juan, E. Coronado, B. Keita, P. de Oliveira, L. Nadjo, F. Secheresse. *Chem.-Eur. J.*, **13**, 3525 (2007); (d) P. Mialane, A. Dolbecq, E. Riviere, J. Marrot, F. Secheresse. *Angew. Chem. Int. Ed.*, **43**, 2274 (2004); (e) P. Mialane, A. Dolbecq, J. Marrot, E. Riviere, F. Secheresse. *Angew. Chem. Int. Ed.*, **42**, 3523 (2003).

[11] (a) H.S. Liu, C.J. Gomez-Garcia, J. Peng, Y.H. Feng, Z.M. Su, J.Q. Sha, L.X. Wang. *Inorg. Chem.*, **46**, 10041 (2007); (b) C.L. Wang, S.X. Liu, C.Y. Sun, L.H. Xie, Y.H. Ren, D.D. Liang, H.Y. Cheng. *J. Mol. Struct.*, **841**, 88 (2007).

[12] (a) C. Pichon, A. Dolbecq, P. Mialane, J. Marrot, E. Riviere, F. Secheresse. *Dalton Trans.*, 71 (2008); (b) C. Pichon, P. Mialane, A. Dolbecq, J. Marrot, E. Riviere, B. Keita, L. Nadjo, F. Secheresse. *Inorg. Chem.*, **46**, 5292 (2007).

[13] J. Fischer, L. Ricard, R. Weiss. *J. Am. Chem. Soc.*, **98**, 3050 (1976).

[14] M. Bösing, I. Loose, H. Pohlmann, B. Krebs. *Chem.-Eur. J.*, **3**, 1232 (1997).

[15] I. Loose, E. Droste, M. Bösing, H. Pohlmann, M.H. Dickman, C. Rosu, M.T. Pope, B. Krebs. *Inorg. Chem.*, **38**, 2688 (1999).

[16] D. Laurencin, R. Villanneau, P. Herson, R. Thouvenot, Y. Jeannin, A. Proust. *Chem. Commun.*, 5524 (2005).

[17] L.H. Bi, T. McCormac, S. Beloshapkin, E. Dempsey. *Electroanalysis*, **20**, 38 (2008).

[18] D. Drewes, E.M. Limanski, M. Piepenbrink, B. Krebs. *Z. Anorg. Allg. Chem.*, **630**, 58 (2004).

[19] I.D. Brown, D. Altermatt. *Acta Crystallogr.*, **B41**, 244 (1985).